Tectono-metamorphic evolution and stratigraphy of the European continental margin involved in the Alpine subduction: New insights from Alpine Corsica, France

Maria Di Rosa, Chiara Frassi, Francesca Meneghini, Michele Marroni, Luca Pandolfi, Alberto De Giorgi

Supplementary Material

Fig. Sm1. Mesoscopic and microscopic aspects of the studied rocks. (a) Macrophotograph of S0+S2 foliation in the Metabreccia Fm. (CPU, Corte area), F2 isoclinal folds and F3 folds in Metabreccia Fm., Corte area (CPU). A.P.2: F2 axial plane; A.P.3: F3 axial plane. (b) Photomicrograph of S1 foliation (S1) preserved within D2 microlithon in the F2 hinge zone of the Metasandstone Fm., PPU, Corte area, sample CM32C. S2: S2 foliation; Wm: white mica; Chl: chlorite. Metabreccia Fm., Corte area (CDU, sample CM24C). (c) cm-sized F3 fold in foliated metagranitoids, Ghisoni area (GHU). (d) Photomicrograph of metagranitoids, Ghisoni area (GHU, sample GHI21). The granoblastic layer consists of recrystallized quartz (Qtz) affected by incipient subgrain rotation recrystallization mechanism. ng: new grain of quartz; og: old grain of quartz; Wm: white mica.

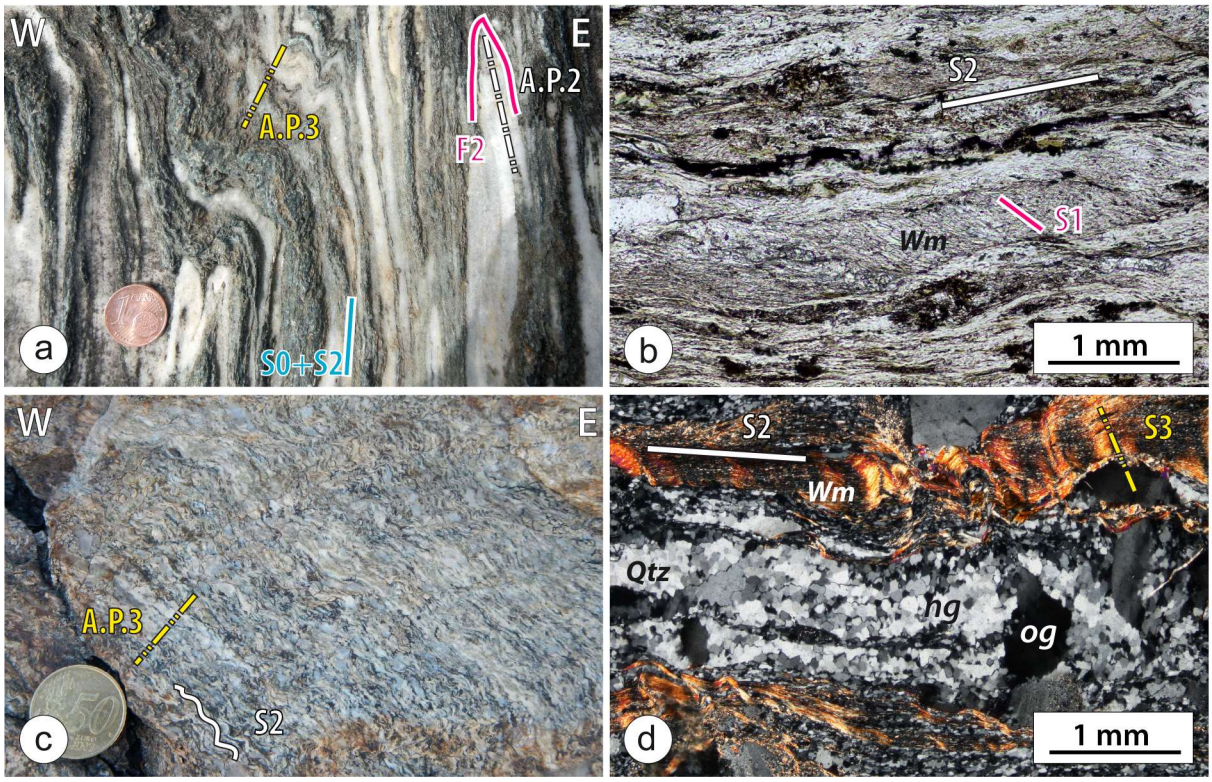

Fig. Sm2. Additional mesoscopic and microscopic pictures of the deformation history of the Lower Units. (a) S–C' fabric in the Detritic Metalimestone Fm., Castiglione–Popolasca Unit, Corte area (C': shear plane; S2: S2 foliation); (b) S-C' microfabric in the Metavolcanic and Metavolcaniclastic Fm., sample CMD51, Ghisoni area; crossed Nicols (C': shear plane; S2: S2 foliation; ulmy: ultramylonite layer); (c) S2 mylonitic foliation in metagranitoids, GHI22, Ghisoni area, crossed Nicols (S2: S2 foliation; Wm: white micas; Qtz: quartz; Pl: plagioclase); (d) σ-type amphibole porphyroclast in the epidote-bearing metagabbros, Ghisoni Unit, sample GHI18, parallel Nicols.

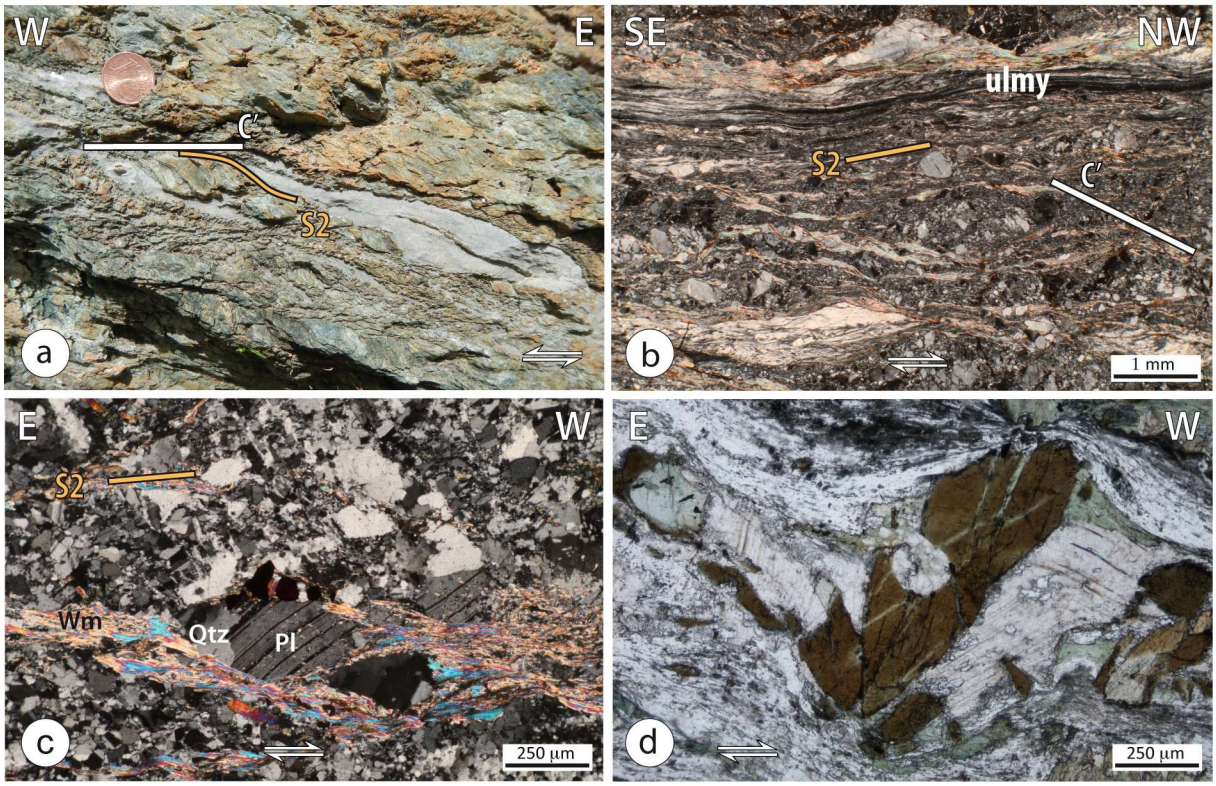

Fig. Sm3. Ternary diagrams showing the proportion in each sample of chlorite (a) and phengite (b) end-members. (c) Si-intensity map acquired with EPMA. (d) *P–T* equilibrium conditions of the three generations of Chl–Phg couples (the error of each cross is ±0.2 GPa and ±30°C). The dots in the maps indicate the sampled microareas from which the *P–T* estimates were obtained.

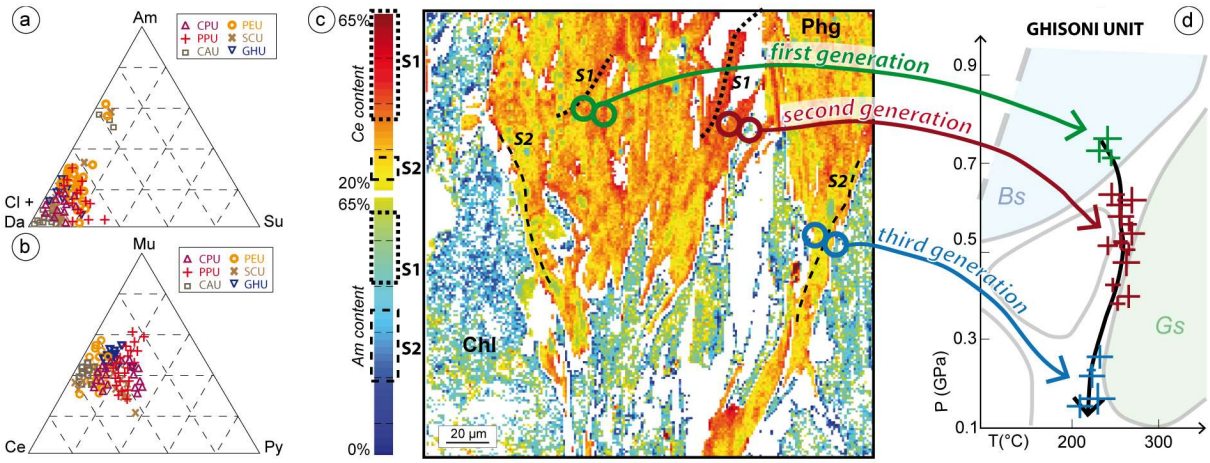

Table Sm1. Representative electron microprobe analysis of the Chl–Phg pairs selected in the samples of metapelites.

Sample	CAU (CMD80A)						PEU (CMD83A)						SCU (CM34B)					
Domain	S1 (P_{peak})		S1 (T_{peak})		S2		S1 (P_{peak})		S1 (T_{peak})		S2		S1 (P_{peak})		S1 (T_{peak})		S2	
Analyse	*Chl70*	*Phg67*	*Chl16*	*Phg43*	*Chl19*	*Phg72*	*Chl2*	*Phg5*	*Chl8*	*Phg1*	*Chl10*	*Phg2*	*Chl1*	*Phg10*	*Chl6*	*Phg8*	*Chl5*	*Phg7*
Wt%																		
SiO_2	25.94	51.57	27.26	52.70	27.68	51.28	23.35	49.63	23.06	47.54	24.23	50.59	24.14	55.90	26.42	50.93	27.33	51.27
TiO_2	0.01	0.05	0.01	0.06	0.01	0.06	0.07	0.18	0.03	0.14	2.26	0.43	0.04	0.06	0.03	0.05	0.04	0.06
Al_2O_3	18.87	26.81	17.31	25.42	17.75	24.07	19.85	22.91	15.70	26.61	16.53	23.08	17.57	24.29	16.47	24.65	16.60	24.22
FeO	21.76	4.02	22.24	4.23	22.69	4.31	31.70	9.43	31.37	8.91	32.07	6.57	27.82	4.53	27.10	5.07	27.08	4.68
MnO	0.42	0.04	0.42	0.04	0.37	0.03	0.79	0.09	0.29	0.05	0.46	0.08	0.25	0.05	0.56	0.06	0.38	0.04
MgO	15.91	3.49	18.58	3.82	18.15	4.19	10.24	2.85	5.01	1.91	7.11	2.37	11.79	3.79	12.32	3.82	12.47	3.71
CaO	0.15	0.07	0.21	0.08	0.13	0.08	0.08	0.06	0.25	0.06	0.10	0.23	0.11	0.03	0.13	0.03	0.13	0.03
Na_2O	0.04	0.04	0.04	0.05	0.03	0.05	0.02	0.15	0.06	0.06	0.02	0.45	0.02	0.02	0.02	0.02	0.02	0.02
K_2O	0.05	10.38	0.08	8.53	0.06	14.34	0.09	10.00	0.31	10.85	0.18	8.68	0.38	8.39	0.41	8.28	0.46	8.27
tot.	83.15	96.46	86.15	94.94	86.87	98.41	86.19	95.30	76.06	96.13	82,96	92.48	82.12	97.05	82.45	92,90	84.51	92.29
Cations																		
Si	2.84	3.42	2.88	3.51	2.91	3.43	2.63	3.44	2.98	3.27	2.85	3.52	2.80	3.62	2.92	3.48	3.04	3.52
Ti	–	–	–	–	–	–	0.01	0.01	–	0.01	0.20	0.02	–	–	–	–	–	–
Al	2.44	2.10	2.16	2.00	2.20	1.90	2.63	1.87	2.39	2.16	2.29	1.89	2.40	1.86	2.23	1.99	2.17	1.96
Fe^{2+}	1.99	0.22	1,97	0.34	1.99	0.24	2.98	0.55	3.39	0.51	3.15	0.38	2.70	0.25	2.60	0.29	2.52	0.27
Mn	0.04	–	0.04	–	0.03	–	0.08	0.01	0.03	–	0.05	0.01	0.03	–	0.05	–	0.04	–
Mg	2.59	0.35	2.94	0.38	2.84	0.42	1.72	0.29	0.97	0.20	1.25	0.25	2.04	0.37	2.11	0.39	2.06	0.38
Ca	0.03	–	0.02	–	0.02	0.01	0.01	–	0.04	–	0.01	0,02	0.01	–	0.02	–	0.01	–
Na	–	–	0.01	0.01	0,01	0.01	–	0.02	0.01	0.01	0.01	0.06	–	–	–	–	–	–
K	0.01	0.88	0.01	0.72	0.01	1.22	0.01	0.88	0.05	0.95	0.03	0.77	0.06	0.69	0.06	0.72	0.07	0.72
sum ox	14	11	14	11	14	11	14	11	14	11	14	11	14	11	14	11	14	11

Sample	CPU (CM22B)						PPU (CM21)						GHU (CMD50D)					
Domain	S1 (P_{peak})		S1 (T_{peak})		S2		S1 (P_{peak})		S1 (T_{peak})		S2		S1 (P_{peak})		S1 (T_{peak})		S2	
Analyse	Chl 757	Phg 269	Chl 856	Phg 55	Chl 26	Phg 136	*Chl 31*	*Phg 18*	*Chl 18*	*Phg 13*	*Chl 12*	*Phg 5*	Chl 24145	Phg 11120	Chl 48	Phg 124	Chl 43	Phg 322
Wt%																		
SiO_2	25.77	50.81	27.22	52.92	28.14	45.36	28.27	48.40	25.58	50.22	30.67	55.27	28.65	49.57	28.19	50.58	28.21	50.08
TiO_2	0.03	0,27	0.03	0.18	0.03	0.23	0.02	0.11	0.03	0.12	0.03	0.21	0.22	0.04	0.03	0.06	0.04	0.04
Al_2O_3	19.68	20.86	22.35	28.77	19.51	22.06	22.61	30.56	20.98	29.77	23.67	28.36	22.94	28.25	22.15	29.18	19.08	29.03
FeO	24.47	4.30	23.58	3.48	24.85	4.19	22.54	3.31	26.91	3.06	19.87	3.48	22.10	4.26	21.70	4.00	22.51	3.61
MnO	0.42	0.02	0.36	0.03	0.36	0.04	0.04	2.29	0.03	2.27	0.03	0.03	0.58	0.04	0.63	0.05	0.60	0.03
MgO	14.94	3.17	13.21	3.65	15.15	2.69	13.99	0.03	13.36	0.03	13.19	3.62	18.03	3.19	17.76	2.83	18.92	2.67
CaO	0.01	0.04	0.01	0.01	0.01	0.03	0.04	0.01	0.04	0.01	0.03	0.02	0.04	0.05	0.05	0.07	0.09	0.05
Na_2O	0.02	0.17	0.02	0.03	0.02	0.07	0.05	0.14	0.05	0.15	0.05	0.04	0.01	0.11	0.03	0.11	0.02	0.12
K_2O	0.05	7.13	0.02	8.21	0.02	7.90	0.68	8.98	0.06	9.01	1.12	8.29	0.01	9.85	0.01	9.87	0.02	10.28
tot.	85.57	86.77	86.8	97.28	88.09	82.57	88.24	93.83	87.04	94.64	88.66	99.32	92.58	95.36	90.55	96.75	89.49	95.91
Cations																		
Si	2.97	3.86	3.04	3.62	3.13	3.69	3.10	3.48	2.91	3.56	3.29	3.69	3.02	3.54	3.04	3.54	3.1	3.55
Ti	–	0.02	–	0,01	–	0.02	–	0.01	–	0.01	–	0.01	0.02	–	–	–	–	–
Al	2.29	1,59	2.50	1.97	2.17	1.79	2.48	2.20	2.39	2.11	2.54	1.89	2.41	2.01	2.39	2.04	2.10	2.06
Fe^{2+}	2.83	0.33	2.64	0.24	2.76	0.34	2.47	0.24	3.06	0.22	2.13	0.23	2.33	0.3	2.34	0.28	2.48	0.26
Mn	0.05	–	0.04	–	0.04	–	–	0.16	–	0.16	–	–	0.06	–	0.07	–	0.07	–
Mg	1.72	0.24	1.48	0.25	1.68	0.22	1.54	–	1.52	–	1.41	0.24	1.90	0.23	1.92	0.20	2.08	0.19
Ca	–	–	–	–	–	–	0.01	0.01	0.01	0.01	0.01	–	–	–	0.01	–	0.01	–
Na	–	0,01	–	–	–	–	0.07	0.65	0.01	0.64	0.12	0.55	–	0.01	–	0.01	–	–
K	0.01	0.54	–	0,56	–	0.64	3.10	3.48	2.91	3.56	3.29	3.69	–	0.7	–	0.69	–	0.73
sum ox	14	11	14	11	14	11	14	11	14	11	14	11	14	11	14	11	14	11

–: below detection limits

Table Sm2 *P–T* estimates for the three generations of Chl–Phg pairs in the six studied units. *P–T* estimates of CPU and PPU are after Di Rosa et al. (2017a). The results (Chl–Phg 1st, 2nd and 3rd generation) obtained with the Chl–Phg-quartz-water multiequilibrium approach (Vidal and Parra, 2000) are compared with classical thermobarometric methods (P_{max} and T_{max}).

	unit	Chl–Phg 1st generation		Chl–Phg 2nd generation		Chl–Phg 3rd generation		P_{max} (Massonne and Schreyer, 1987)	T_{max}
		D1 PHASE				D2 PHASE			
		T **(°C)**	***P*** **(GPa)**	***T*** **(°C)**	***P*** **(GPa)**	***T*** **(°C)**	***P*** **(GPa)**	***P*** **(GPa)**	***T*** **(°C)**
CIMA PEDANI area	CAU	176–262	1.04–0.82	393–455	0.76–0.63	310–247	0.45–0.33	1.08	470 (Hillier and Velde, 1991)
	PEU	280–360	1.35–0.80	440–435	0.75–0.45	351–237	0.35–0.23	1.25	452 (Cathelineau, 1988)
	SCU	277–280	1.34–0.90	435–388	0.83–0.51	312–278	0.31–0.26	0.81	401 (Lanari et al., 2014)
CORTE area	PPU	200–240	1.04–0.75	340–400	0.80–0.51	300–240	0.30–0.23	1.19	344 (Lanari et al., 2014)
	CPU	250–330	1.22–1.00	350–320	0.80–0.56	310–230	0.36–0.25	1.26	350 (Lanari et al., 2014)
GHISONI area	GHU	245–250	0.81–072	263–243	0.68–0.39	228–209	0.30–0.13	0.92	272 (Lanari et al., 2014)

References

Cathelineau, M., 1988. Cation site occupancy in chlorites and illites as a function of temperature. Clay Minerals 23, 471–485.

Di Rosa, M., De Giorgio, A., Marroni, M., Vidal, O., 2017. Syn-convergence exhumation of continental crust: evidence from structural and metamorphic analysis of the Monte Cecu area, Alpine Corsica (Northern Corsica, France). Geol. J. 52, 019-937.

Hillier, S., Velde, B., 1991. Octahedral occupancy and the chemical composition of diagenetic (low-temperature) chlorites. Clay Minerals 26, 146–168.

Lanari, P., Wagner, T., Vidal, O. 2014. A thermodynamic model for di–trioctahedral chlorite from experimental and natural data in the system MgO–FeO–Al_2O_3–SiO_2–H_2O: applications to *P–T* sections and geothermometry. Contrib. Mineral. Petrol. 167. doi:10.1007/s00410-014-0968-8.

Massonne, H.J., Schreyer, W., 1987. Phengite geobarometry based on the limiting assemblage with K-feldspar, phlogopite, and quartz. Contrib. Mineral. Petr. 96, 212–224.

Vidal, O., Parra, T., 2000. Exhumation paths of high-pressure metapelites obtained from local equilibria for chlorite–phengite assemblage. Geol. J. 35, 139–161.